



American Society of Hematology
 2021 L Street NW, Suite 900,
 Washington, DC 20036
 Phone: 202-776-0544 | Fax 202-776-0545
 editorial@hematology.org

Kinase-inactivated CDK6 preserves the long-term functionality of adult hematopoietic stem cells

Tracking no: BLD-2023-021985R2

Isabella Mayer (University of Veterinary Medicine, Austria) Eszter Doma (University of Veterinary Medicine, Austria) Thorsten Klampfl (University of Veterinary Medicine Vienna, Austria) Michaela Prchal-Murphy (Veterinary University of Vienna, Austria) Sebastian Kollmann (University of Veterinary Medicine, Austria) Alessia Schirripa (University of Veterinary Medicine, Austria) Lisa Scheiblecker (University of Veterinary Medicine Vienna, Austria) Markus Zojer (University of Veterinary Medicine, Austria) Natalia Kunowska (University of Graz, Austria) Lea Gebrail (University of Veterinary Medicine, Austria) Lisa Shaw (Medical University Vienna, Austria) Ulrike Mann (Medical University of Vienna, Austria) Alex Farr (Medical University of Vienna, Austria) Reinhard Grausenburger (University of Veterinary Medicine Vienna, Austria) Gerwin Heller (Medical University of Vienna, Austria) Eva Zebedin-Brandl (medical university, Austria) Matthias Farlik (Medical University of Vienna, Austria) Marcos Malumbres (Vall d'Hebron Institute of Oncology (VHIO) and ICREA, Spain) Veronika Sexl (University of Innsbruck, Austria) Karoline Kollmann (University of Veterinary Medicine Vienna, Austria)

Abstract:

Hematopoietic stem cells (HSCs) are characterized by the ability to self-renew and to replenish the hematopoietic system. The cell-cycle kinase cyclin dependent-kinase 6 (CDK6) regulates transcription, whereby it has both kinase-dependent and kinase-independent functions. We here describe the complex role of CDK6, balancing quiescence, proliferation, self-renewal and differentiation in activated HSCs. Mouse HSCs expressing kinase-inactivated CDK6 show enhanced long-term repopulation and homing, whereas HSCs lacking CDK6 have impaired functionality. The transcriptomes of basal and serially transplanted HSCs expressing kinase-inactivated CDK6 exhibit an expression pattern dominated by HSC quiescence and self-renewal, proposing a concept where MAZ and NFY-A are critical CDK6 interactors. Pharmacologic kinase inhibition with a clinically used CDK4/6 inhibitor in murine and human HSCs validated our findings and resulted in increased repopulation capability and enhanced stemness. Our findings highlight a kinase-independent role of CDK6 in long-term HSC functionality. CDK6 kinase inhibition represents a possible strategy to improve HSC fitness.

Conflict of interest: No COI declared

COI notes:

Preprint server: No;

Author contributions and disclosures: Conceptualization, I.M.M., T.K., E.D., V.S., K.K.; formal analysis, T.K., M.Z., R.G., G.H.; performing experiments I.M.M., E.D., S.K., L.S., M.P-M., A.S., M.F.; technical support U.M., L.E.S., N.K; resources: M.M.; A.F., E.Z-B.; writing, I.M.M., E.D., T.K., K.K.; supervision, V.S., K.K.

Non-author contributions and disclosures: No;

Agreement to Share Publication-Related Data and Data Sharing Statement: Low-input RNA-seq data are available at GEO under accession number E-MTAB-13145 or with the link <https://www.ebi.ac.uk/biostudies/arrayexpress/studies/E-MTAB-13145?key=ab2083d3-92c0-4cf9-ab87-cb4bfb5fb8f7>. ScRNA-seq data of Cdk6+/+, Cdk6KM/KM and Cdk6-/- LSK cells are available at GEO under accession number E-MTAB-13149 or the link <https://www.ebi.ac.uk/biostudies/arrayexpress/studies/E-MTAB-13149?key=1c62daa4-fe2b-442a-a1e0-9840d5c0c00a>. ScRNA-seq data of Palbociclib or Ctrl pre-treated LSK cell are available at GEO under accession number E-MTAB-13268 or the link <https://www.ebi.ac.uk/biostudies/arrayexpress/studies/E-MTAB-13268?key=6f57d2b2-99d3-4c6b-b088-2b7f9fbc6967>.

Clinical trial registration information (if any):

1 **Kinase-inactivated CDK6 preserves the long-term functionality**
2 **of adult hematopoietic stem cells**

3
4 Isabella M. Mayer¹, Eszter Doma¹, Thorsten Klampfl¹, Michaela Prchal-Murphy¹, Sebastian
5 Kollmann¹, Alessia Schirripa¹, Lisa Scheiblecker¹, Markus Zojer¹, Natalia Kunowska², Lea
6 Gebrail¹, Lisa E. Shaw³, Ulrike Mann³, Alex Farr⁴, Reinhard Grausenburger¹, Gerwin Heller⁵,
7 Eva Zebedin-Brandl⁶, Matthias Farlik³, Marcos Malumbres⁷⁻⁹, Veronika Sexl^{1,10}, Karoline
8 Kollmann^{1,*}

9
10 *¹University of Veterinary Medicine Vienna, Department of Biological Sciences and*
11 *Pathobiology, Pharmacology and Toxicology, 1210 Vienna, Austria*

12 *²University of Graz, Pharmaceutical Chemistry, Institute of Pharmaceutical Sciences, 8010*
13 *Graz, Austria*

14 *³Medical University of Vienna, Department of Dermatology, 1090 Vienna Austria*

15 *⁴Medical University of Vienna, Department of Obstetrics and Gynecology, 1090 Vienna*
16 *Austria*

17 *⁵Medical University of Vienna, Department of Medicine I, Clinical Division of Oncology,*
18 *1090 Vienna, Austria*

19 *⁶Medical University of Vienna, Institute of Pharmacology, Centre of Physiology and*
20 *Pharmacology, 1090 Vienna Austria*

21 *⁷Vall d'Hebron Institute of Oncology (VHIO), Cancer Cell Cycle group, 08035 Barcelona,*
22 *Spain*

23 *⁸Spanish National Cancer Research Center (CNIO), Cell Division and Cancer group, 28029*
24 *Madrid, Spain.*

25 *⁹ICREA, 08010 Barcelona, Spain*

26 *¹⁰University of Innsbruck, 6020 Innsbruck, Austria*

27 **Lead contact*

28
29 ***Correspondence:** karoline.kollmann@vetmeduni.ac.at

30
31 Low-input RNA-seq data are available at GEO under accession number E-MTAB-13145 or
32 with the link <https://www.ebi.ac.uk/biostudies/arrayexpress/studies/E-MTAB->

33 13145?key=ab2083d3-92c0-4cf9-ab87-cb4bfb5fb8f7. ScRNA-seq data of Cdk6+/+,
34 Cdk6KM/KM and Cdk6-/- LSK cells are available at GEO under accession number E-
35 MTAB-13149 or the link [https://www.ebi.ac.uk/biostudies/arrayexpress/studies/E-MTAB-](https://www.ebi.ac.uk/biostudies/arrayexpress/studies/E-MTAB-13149?key=1c62daa4-fe2b-442a-a1e0-9840d5c0c00a)
36 [13149?key=1c62daa4-fe2b-442a-a1e0-9840d5c0c00a](https://www.ebi.ac.uk/biostudies/arrayexpress/studies/E-MTAB-13149?key=1c62daa4-fe2b-442a-a1e0-9840d5c0c00a). ScRNA-seq data of Palbociclib or Ctrl
37 pre-treated LSK cell are available at GEO under accession number E-MTAB-13268 or the
38 link [https://www.ebi.ac.uk/biostudies/arrayexpress/studies/E-MTAB-13268?key=6f57d2b2-](https://www.ebi.ac.uk/biostudies/arrayexpress/studies/E-MTAB-13268?key=6f57d2b2-99d3-4c6b-b088-2b7f9fbc6967)
39 [99d3-4c6b-b088-2b7f9fbc6967](https://www.ebi.ac.uk/biostudies/arrayexpress/studies/E-MTAB-13268?key=6f57d2b2-99d3-4c6b-b088-2b7f9fbc6967).

40

41 **Running title:** Kinase-inactivated CDK6 maintains HSC self-renewal

42

43 **Key words:** HSC; self-renewal; CDK6; MAZ; kinase inactive;

44 **Abstract**

45 Hematopoietic stem cells (HSCs) are characterized by the ability to self-renew and to
46 replenish the hematopoietic system. The cell-cycle kinase cyclin dependent-kinase 6 (CDK6)
47 regulates transcription, whereby it has both kinase-dependent and kinase-independent
48 functions. We here describe the complex role of CDK6, balancing quiescence, proliferation,
49 self-renewal and differentiation in activated HSCs. Mouse HSCs expressing kinase-
50 inactivated CDK6 show enhanced long-term repopulation and homing, whereas HSCs lacking
51 CDK6 have impaired functionality. The transcriptomes of basal and serially transplanted
52 HSCs expressing kinase-inactivated CDK6 exhibit an expression pattern dominated by HSC
53 quiescence and self-renewal, proposing a concept where MAZ and NFY-A are critical CDK6
54 interactors. Pharmacologic kinase inhibition with a clinically used CDK4/6 inhibitor in
55 murine and human HSCs validated our findings and resulted in increased repopulation
56 capability and enhanced stemness. Our findings highlight a kinase-independent role of CDK6

57 in long-term HSC functionality. CDK6 kinase inhibition represents a possible strategy to
58 improve HSC fitness.

59

60 **Key Points**

61

62 - Inhibiting CDK6 kinase function enhances long-term HSC functionality

63

64 - Kinase-inactivated CDK6 and MAZ influence HSC maintenance

65

66

67

68 **Introduction**

69 HSCs are rare components of the adult bone marrow (BM), where they preserve the
70 hematopoietic pool by self-renewal and differentiation¹⁻³. Hematopoietic stem cell
71 transplantation (HSCT) is an essential medical procedure for various hematological diseases⁴⁻
72 ⁶. Although HSCT is a life-saving process, it comes with several limitations due to graft-
73 versus-host disease or relapse^{4,5}. The objective is to use most functional and fittest HSCs for a
74 successful HSCT.

75 CDK6 controls the exit from the G₁ phase of the cell cycle in all cells. The cell cycle is
76 triggered by binding of CDK6 to D-type cyclins, which activates the kinase function of CDK6
77 and leads to phosphorylation of the retinoblastoma protein (Rb). Subsequent E2F-mediated
78 transcription causes the cells to exit G₁ and enter the S phase⁷. In addition to phosphorylating
79 Rb, CDK6 regulates the transcription of a range of genes in healthy and malignant cells. It
80 does not itself bind to DNA but interacts with a plethora of transcription factors, either in a
81 kinase-dependent or in a kinase-independent manner⁸⁻¹³. Using transgenic CDK6 animal
82 models, has been instrumental in our understanding of the complex interplay of the kinase-

83 dependent and -independent functions of CDK6 in HSPCs^{14,15}. However, we do not
84 understand how CDK6 controls the fate of these cells.

85 We now report that inactivation of the kinase function of CDK6 leads to an enriched pool of
86 quiescent HSCs with a long-term capacity to repopulate the hematopoietic system. We also
87 show that HSCs containing a kinase-inactivated version of CDK6 retain certain features of
88 stem cells that are lost when the HSCs lack CDK6. Our transcriptomics data provide a model
89 to explain how CDK6 stimulates or represses various transcriptional networks to control the
90 fate of HSCs.

91

92 **Methods**

93 *Serial BM transplantation assays*

94 5×10^6 BM of *Cdk6*^{+/+}, *Cdk6*^{-/-} or *Cdk6*^{KM/KM} donor cells were transplanted intravenously (*i.v.*)
95 into lethally irradiated CD45.1⁺ recipients. The long-term repopulation capacities were
96 evaluated after twelve weeks following transplantation by flow cytometry. 5×10^6 CD45.2⁺
97 donor BM cells were re-injected in lethally irradiated CD45.1⁺ recipient mice for up to four
98 rounds.

99 *Single and repetitive pI:pC injections*

100 Mice were injected once intraperitoneally (*i.p.*) with 10 mg/kg polyinosinic:polycytidylic acid
101 (pI:pC). Control mice were injected with the same volume of PBS. Mice were opened 18
102 hours post-treatment and HSC compartment was analysed.

103 For repetitive analysis, mice were serially injected *i.p.* in every second day (three times total)
104 with 10 mg/kg pI:pC or PBS. Mice were opened 2 days post 3rd injection.

105 All procedures and breeding were approved by the Ethics and Animal Welfare Committee of
106 the University of Veterinary Medicine, Vienna in accordance with the University's guidelines
107 for Good Scientific Practice and authorized by the Austrian Federal Ministry of Education,
108 Science and Research (BMMWF-68.205/0093-WF/V/3b/2015, 2022-0.404.452, BMMWF-
109 68.205/0112-WF/V/3b/2016, BMBWF-68.205/0103-WF/V/3b/2015 (TP), 2023-0.108.862) in
110 accordance with current legislation. The experimental protocols involving human cord blood
111 samples was approved by the Ethics Committee of the Medical University of Vienna
112 (EK1553/2014).

113 Other methods are described in detail in supplemental Methods, available on the Blood
114 website

116 **Results**

117 **CDK6 shapes the HSC transcriptomic landscape in a kinase -dependent and -**
118 **independent manner**

119 To understand the contribution of kinase-dependent and -independent functions of CDK6 in
120 HSCs, we made use of a kinase-inactivated CDK6 K43M knock-in mouse model
121 (*Cdk6*^{KM/KM})¹⁴, which was compared to CDK6 wild type (*Cdk6*^{+/+}) and CDK6 knockout mice
122 (*Cdk6*^{-/-})¹⁵. HSPC fractions of *Cdk6*^{+/+} and *Cdk6*^{KM/KM} mice showed comparable CDK6 protein
123 levels (**Fig. S1A-C**). Although BM cellularity was reduced in *Cdk6*^{KM/KM} and *Cdk6*^{-/-} mice,
124 LSK cell numbers remained unaffected (**Fig. 1A, S1D**). HSC cell numbers were increased and
125 multipotent progenitor 3/4 (MPP3/4) cell numbers are reduced in the *Cdk6*^{KM/KM} mice
126 compared to *Cdk6*^{+/+} mice, whereas *Cdk6*^{-/-} mice showed reduced MPP2 cell numbers
127 compared to *Cdk6*^{+/+} mice (**Fig. 1A**). *Cdk6*^{KM/KM} and *Cdk6*^{-/-} mice showed significantly
128 increased percentage of the HSC subfraction, while the percentage of LSK and MPP1-4 cells
129 remained unaltered irrespective of the genotype (**Fig. S1E-F**).

130 To determine underlying transcriptional changes in the HSC compartment, we performed
131 high-resolution 10X genomics single-cell RNA-seq (scRNA-seq) of steady-state BM LSK
132 cells. Data integration identified 11 individual cell clusters, which we annotated according to
133 published marker gene expression (**Fig. 1B, S1G**)^{16,17}. Differences in cluster sizes were
134 notable between *Cdk6*^{KM/KM} and *Cdk6*^{-/-} compared to *Cdk6*^{+/+} cells (**Fig. S1H**). In line with the
135 known cell cycle function of CDK6^{7,14,15}, the “cell cycle clusters” in *Cdk6*^{-/-} and *Cdk6*^{KM/KM}
136 samples were smaller compared to the *Cdk6*^{+/+} cluster. Flow cytometry analysis of *ex vivo*
137 and cultivated *Cdk6*^{-/-} and *Cdk6*^{KM/KM} LSK or HSC/MPP1 cells verified reduced proliferation
138 (**Fig. S1I-J**).

139 The HSPC cluster of the scRNA-seq experiment encompassed approximately 20% of all LSK
140 cells (**Fig. 1B**). To better identify transcriptional patterns in more defined HSPCs, we re-
141 integrated the HSPC cluster and annotated dormant HSCs and differentiation-prone cell states
142 based on published marker genes (**Fig. 1C, S1K**)^{16,17}. We found nine HSPC subclusters which
143 exhibited transcriptional alterations particularly in the *Cdk6*^{KM/KM} mutant setting when
144 compared to *Cdk6*^{+/+} or *Cdk6*^{-/-} cells. All *Cdk6*^{KM/KM} clusters show a more pronounced effect
145 in size compared to *Cdk6*^{-/-} clusters, except the cell cycle cluster. We identified opposing
146 effects of *Cdk6*^{KM/KM} and *Cdk6*^{-/-} cells within the myeloid (Myel), lymphoid (Lym) and
147 interferon (IFN) HSPC subclusters. *Cdk6*^{KM/KM} and *Cdk6*^{-/-} samples showed increased dormant
148 HSCs to a similar extent as shown in **Fig.1A (Fig. 1D)**. Strikingly, *Cdk6*^{KM/KM} HSCs
149 displayed a unique transcriptional pattern leading to an alternative cluster formation (**Fig. 1E**).
150 Differential gene expression analysis of the dormant HSC subcluster unmasked common and
151 unique up- and downregulated genes in *Cdk6*^{KM/KM} and *Cdk6*^{-/-} compared to *Cdk6*^{+/+} cells (**Fig.**
152 **1F**). *Cdk6*^{KM/KM} HSCs showed on average a reduced expression of a proliferation gene
153 signature (PSig)¹⁸ compared to *Cdk6*^{-/-} and *Cdk6*^{+/+} cells (**Fig. 1G**). *Cdk6*^{-/-} cells showed a
154 stronger expression of the quiescence associated signature (Qsig)¹⁸ compared to *Cdk6*^{KM/KM}
155 and *Cdk6*^{+/+} cells. This result aligns with our previously published data, highlighting that the
156 absence of CDK6 impairs HSC exit from their quiescent state, along with decreased response
157 to HSC-specific stress conditions¹³. These data led us to speculate that *Cdk6*^{KM/KM} HSCs
158 respond differently to HSC specific stress challenge compared to *Cdk6*^{-/-} HSCs. Kinase-
159 inactivated CDK6 fails to phosphorylate, despite the protein being present, which may block
160 other kinases that compensate in a CDK6-deficient setting.

161

162 **Kinase-inactivated CDK6 maintains HSPC potential upon long-term challenge**

163 The transcriptional changes found in *Cdk6*^{KM/KM} HSCs point towards alterations in interferon
164 (IFN)-response and activation. We thus injected mice with a single dose of
165 polyinosinic:polycytidylic acid (pI:pC) to analyze the activation response in a short-term
166 setting (**Fig. S2A**). To control for the induction of Sca-1 expression by the IFN-STAT1 axis,
167 we decided on an alternative flow cytometry gating strategy including the CD86 marker¹⁹.
168 Lineage⁻ c-kit⁺ CD86⁺ cell numbers are similar between the three genotypes upon pI:pC
169 treatment. (**Fig. S2B**). As under steady state conditions, HSC/MPP1-2 cell numbers were
170 significantly higher in *Cdk6*^{KM/KM} compared to *Cdk6*^{+/+} mice. This was not detected for the
171 *Cdk6*^{-/-} mice (**Fig. S2C**). *Cdk6*^{-/-} HSC/MPP1 cells showed reduced G₁ cell cycle entry upon
172 single pI:pC stimulation, in line with published data¹³ (**Fig. S2D**).

173 To test how *Cdk6*^{KM/KM} cells respond to multiple inflammation associated challenges, we
174 performed serial pI:pC injections followed by serial plating assays to study long-term self-
175 renewal (**Fig. 2A**).

176 Serial pI:pC injections resulted in a decreased BM cellularity in *Cdk6*^{-/-} and *Cdk6*^{KM/KM} mice
177 compared to *Cdk6*^{+/+} mice along with decreased *Cdk6*^{-/-} LK⁺CD86⁺ and HSC/MPP1 cell
178 numbers (**Fig. 2B, S2E**). *Cdk6*^{KM/KM} cells displayed intermediate numbers. MPP2-4 cells
179 remained unchanged irrespective of the genotype (**Fig. S2F**). A higher percentage of *Cdk6*^{-/-}
180 and *Cdk6*^{KM/KM} HSC/MPP1 cells remained in the G₀ and G₁ cell cycle phases (**Fig. 2C**). Our
181 experimental setting was completed by serially plating BM cells into methylcellulose (**Fig.**
182 **2A**). Serial BM cell plating revealed significantly elevated *Cdk6*^{KM/KM} LSK cell numbers. In
183 contrast, *Cdk6*^{-/-} cells showed reduced LSK cell numbers and even more drastically reduced
184 total cell numbers compared to *Cdk6*^{+/+} and *Cdk6*^{KM/KM} cells (**Fig. 2D-E, S2G**). *Cdk6*^{KM/KM}
185 colonies displayed an overall reduction in differentiated cells compared to *Cdk6*^{+/+} and *Cdk6*^{-/-}
186 controls upon serial plating, yet *Cdk6*^{KM/KM} cells were still able to produce myeloid and
187 lymphoid colonies (**Fig. S2H**). The short- and long-term pI:pC data suggest that kinase-

188 inactivated CDK6 mimics full loss of CDK6 in regards to cell cycle, which can be seen most
189 prominently in a short-term activation setting. However, in a repetitive activation setting,
190 where long-term stem cell properties come into account, kinase-inactivated CDK6 maintained
191 LSK numbers, while loss of CDK6 led to reduced LSK cell numbers. The advantage of
192 $Cdk6^{KM/KM}$ HSCs comes with only mild expenses regarding the differentiation potential.

193 Kinase-inactivated CDK6 enhances HSC homing and self-renewal

194 *Angpt1* was one of the top upregulated genes in $Cdk6^{KM/KM}$ compared to $Cdk6^{+/+}$ and $Cdk6^{-/-}$
195 cells from the dormant HSC subcluster (**Fig. 3A**). As *Angpt1/Tie2* is a critical signalling
196 component for HSC quiescence and homing^{20,21}, we tested whether kinase-independent
197 functions of CDK6 affect homing and migration of HSCs (**Fig. S3A**). Sorted LSK cells were
198 plated in a transwell system including stromal cell-derived factor 1 α (SDF-1 α) as an
199 attractant. No changes in migration of the total LSK compartment was observed. When
200 analyzing HSC/MPP1 cells, $Cdk6^{KM/KM}$ cells migrated significantly more than $Cdk6^{-/-}$
201 HSC/MPP1 cells *in vitro*. Therefore we performed an *in vivo* homing assay. We injected
202 CD45.2⁺ LSK cells of $Cdk6^{+/+}$, $Cdk6^{-/-}$ and $Cdk6^{KM/KM}$ mice *i.v.* into CD45.1⁺ recipient mice
203 (**Fig. 3B**). Injected CD45.2⁺ LSK and MPP2-4 progenitor cells were similarly present in the
204 BM irrespective of the genotype 18 hours thereafter (**Fig. 3C, S3B**). In contrast, significantly
205 more $Cdk6^{KM/KM}$ HSC/MPP1 cells homed to the BM compared to $Cdk6^{+/+}$ and $Cdk6^{-/-}$
206 HSC/MPP1 cells.

207 Self-renewal and homing are processes involved in HSC engraftment. To assess the
208 repopulation capacity of $Cdk6^{KM/KM}$ HSC/MPP1 cells we serially transplanted BM cells from
209 CD45.2⁺ $Cdk6^{+/+}$, $Cdk6^{-/-}$ and $Cdk6^{KM/KM}$ mice into lethally irradiated CD45.1⁺ recipient mice
210 (**Fig. 3D**). From the 2nd round of transplantation onwards, we identified significantly higher
211 numbers of donor-derived $Cdk6^{KM/KM}$ LSK cells compared to $Cdk6^{+/+}$ and $Cdk6^{-/-}$ LSK cells

212 **(Fig. 3E-F)**. This effect was even more pronounced for the HSC/MPP1 cell compartment
213 **(Fig. 3G)**. In contrast to *Cdk6*^{KM/KM} cells, *Cdk6*^{-/-} LSK and HSC/MPP1 cells significantly
214 declined over serial rounds of transplantation. *Cdk6*^{KM/KM} MPP2-4 progenitor cells displayed
215 higher percentages of BM engraftment compared to *Cdk6*^{-/-} MPP2-4 cells within all
216 transplantation rounds **(Fig. S3C)**. No significant differences in the MPP2-4 cells were
217 observed between *Cdk6*^{KM/KM} and CDK6 wild type cells.

218 Comparable percentages of myeloid and lymphoid cells were found upon repopulation of
219 *Cdk6*^{+/+} and *Cdk6*^{KM/KM} cells in the long-term transplantation setting **(Fig. 3H)**. Of note, *Cdk6*
220 ^{-/-} cells showed a shift from the myeloid to the lymphoid lineage, with the strongest effect
221 observed in the 2nd serial transplantation round. This data is in line with the enhanced
222 lymphoid HSPC subcluster identified by the scRNA-seq data **(Fig. 1D)**. No significant
223 alterations were detected in the composition of the peripheral blood **(Fig. S3D)**. To further
224 investigate the functionality of CDK6 kinase-inactivated HSC/MPP1 cells, we performed
225 competitive transplantation assays with *Cdk6*^{KM/KM} or *Cdk6*^{+/+} BM cells **(Fig. 3I)**. *Cdk6*^{KM/KM}
226 HSC/MPP1 cells showed a competitive advantage compared to control counterparts **(Fig. 3J)**.
227 No major differences in the MPP2-4 fractions and LSK cells between *Cdk6*^{+/+} and *Cdk6*^{KM/KM}
228 were observed **(Fig. S3F-G)**. These results highlight a specific role for kinase-inactivated
229 CDK6 in the repopulation ability of HSCs, which is not mimicked by full loss of CDK6.
230 *Cdk6*^{KM/KM} HSCs balance proliferation, differentiation, and self-renewal by a unique
231 transcriptional regulation.

232 **Kinase-inactivated CDK6 balances quiescent and activated transcriptional programs of** 233 **long-term HSCs**

234 To gain deeper insights into how kinase-inactivated CDK6 protects HSCs during long-term
235 challenge, we performed low-input RNA-seq of flow cytometry sorted serially transplanted

236 (2nd round) HSC/MPP1 cells (**Fig. 4A**). *Cdk6*^{KM/KM} and *Cdk6*^{-/-} cells showed unique and
237 common transcriptional changes (**Fig. 4B**). As observed in the scRNA-seq analysis, we
238 identified a CDK6 kinase-inactivated, kinase-dependent and CDK6 loss gene set. We first
239 defined gene sets associated with HSC quiescence or HSC activation (**Fig S4A**)²². *Cdk6*^{KM/KM}
240 and *Cdk6*^{+/+} HSC/MPP1 cells displayed a positive enrichment of the quiescent stem cell gene
241 set compared to *Cdk6*^{-/-} HSC/MPP1 cells (**Fig. 4C**). This finding reflected the reduced
242 engraftment potential of the *Cdk6*^{-/-} HSC/MPP1 cells over *Cdk6*^{KM/KM} and *Cdk6*^{+/+}
243 HSC/MPP1 cells (**Fig. 3G**). A significant negative enrichment of the activation stem cell gene
244 set was identified for *Cdk6*^{KM/KM} and *Cdk6*^{-/-} HSC/MPP1 cells compared to *Cdk6*^{+/+}
245 HSC/MPP1 cells, which aligns with the proliferation associated gene signature from the
246 dormant HSC cluster (**Fig. 4D, 1G**). These results highlight the importance of kinase-
247 independent effects of CDK6 in maintaining quiescent gene expression patterns, which
248 becomes critical under HSC long-term behavior. The regulation of the *Cdk6*^{KM/KM} and *Cdk6*^{-/-}
249 quiescent genes is formerly evident under homeostasis, where we identified a different
250 transcriptional pattern of the dormant *Cdk6*^{KM/KM} HSC subcluster (**Fig. 1E-G**).

251 The CDK6 protein lacks a DNA-binding domain and acts as a transcriptional cofactor^{7-9,11,14}.
252 To understand how CDK6 regulates HSC self-renewal and maintenance, we performed a
253 transcription factor motif analysis in promoter regions of the differentially expressed
254 activation signature genes between kinase-inactivated CDK6 and wild type CDK6.

255 NFY and E2F motifs have been revealed as top hits (**Fig. 4E**). When performing a motif
256 enrichment analysis for the comparison of *Cdk6*^{-/-} to *Cdk6*^{+/+} cells, we identified a similar
257 pattern than *Cdk6*^{KM/KM} mutant compared to *Cdk6*^{+/+} cells (**Fig. 4F**). These results validated
258 the canonical cell cycle function of CDK6. Our results confirmed published data of NFY-A,
259 showing that it is a critical factor in proliferating HSCs.

260 We recently described that CDK6 phosphorylates NFY-A at serine position S325 in
261 transformed BCR/ABL⁺ cells. Thereby NFY-A is activated for its transcriptional function¹⁰.
262 To validate a CDK6-NFY-A interaction in hematopoietic progenitor cells, we took advantage
263 of our recently established HPC^{LSK} system and generated stem/progenitor cell lines from
264 *Cdk6*^{+/+}, *Cdk6*^{-/-} and *Cdk6*^{KM/KM} mice.²³ Subcellular fractionation analysis revealed that
265 kinase-inactivated and wild type CDK6 protein was comparable in the chromatin and
266 cytoplasmic fractions (**Fig. 4G**) in HPC^{LSK} cells, predicting that kinase-inactivated CDK6
267 interacts with the chromatin in a similar manner as wild type CDK6. Co-immunoprecipitation
268 (Co-IP) confirmed the protein-protein interaction of CDK6 and NFY-A in *Cdk6*^{+/+} and
269 *Cdk6*^{KM/KM} HPC^{LSK} cells (**Fig. 4H**). To better understand the significance of this interaction,
270 we performed NFY-A shRNA knockdown experiments with *Cdk6*^{+/+}, *Cdk6*^{-/-} and *Cdk6*^{KM/KM}
271 HPC^{LSK} cells. Upon NFY-A knockdown, *Cdk6*^{KM/KM} HPC^{LSK} cells responded with an
272 increased cell death compared to *Cdk6*^{+/+} and *Cdk6*^{-/-} cells (**Fig. S4B-C**). This data is in line
273 with previous reports that NFY-A loss induces apoptosis and CDK6 kinase activity is needed
274 to antagonize p53-responses^{10,24,25}.

275

276 Kinase-inactivated CDK6 and MAZ influence HSC maintenance

277 To identify kinase-inactivated CDK6 interactors maintaining quiescence, we combined motif
278 enrichment analysis with a CDK6 IP-mass spectrometry experiment. We performed motif
279 enrichment analysis of *Cdk6*^{KM/KM} and *Cdk6*^{-/-} deregulated genes compared to *Cdk6*^{+/+} within
280 the quiescent stem cell gene set from and defined *Cdk6*^{KM/KM} specific motifs (**Fig. 5A-B,**
281 **S5A**). We performed a nuclear CDK6 immunoprecipitation followed by mass spectrometry
282 analysis with the hematopoietic progenitor cell line HPC-7²⁶ (**Fig. 5C**). An overlap of this
283 data with the *Cdk6*^{KM/KM} specific motifs highlighted ZNF148, RUNX1 and myc-associated

284 zinc finger protein (MAZ) as strongest interactors. The MAZ-CDK6 interaction was validated
285 by proximity ligation assays in *Cdk6*^{+/+} and *Cdk6*^{KM/KM} HSC/MPP1 cells (**Fig. 5D**).

286 To assess whether CDK6 and MAZ interplay at chromatin, we re-analyzed publicly available
287 ChIP-seq data sets from transformed B-cells.^{10,27} 9501 binding sites were identified as
288 common peaks for CDK6 and MAZ (**Fig. 5E-F**). The associated CDK6-MAZ bound genes
289 enriched for pathways related to chromatin modification, transcriptional regulation, and
290 apoptotic signalling (**Fig. S5B**).

291 The overlap of CDK6-MAZ binding sites with *Cdk6*^{KM/KM} genes upregulated in the HSC
292 subcluster of **Figure 1E** identified that approximately 50% of all genes display a common
293 binding site (**Fig. 5G**). Among these 282 genes are several known HSC mediators (**Fig.**
294 **5H**)^{16,17,22,28}.

295 Palbociclib (CDK4/6 kinase inhibitor) treatment did not affect MAZ interaction with the
296 promoters of *Mlec*, *Fosb* and *Hmgb2* in *Cdk6*^{+/+} HPC^{LSK} cells (**Fig. S5C**) but CDK6 kinase
297 activity influences the transcription of *Mlec* and *Fosb* which is abrogated by MAZ
298 knockdown (siMAZ) (**Fig. S5D**).

299 MAZ knockdown was performed in sorted LSK cells from *Cdk6*^{+/+} and *Cdk6*^{KM/KM} mice (**Fig.**
300 **5I, S5E**). *Cdk6*^{KM/KM} cells responded with a decrease in HSC/MPP1 cells compared to
301 controls (**Fig. 5J-K**). Palbociclib treated *Cdk6*^{+/+} LSKs with siMAZ gave comparable results
302 and reduced HSC/MPP1 numbers. The LSK cell fraction remained unaltered in the different
303 conditions (**Fig. S5F**). In summary, this data point at a critical role of the kinase-inactivated
304 CDK6-MAZ axes for HSC maintenance.

305

306 **CDK4/6 kinase inhibition protects HSC fitness**

307 We made use of Palbociclib to evaluate its effects on *Cdk6*^{+/+} LSK cells by using 10X
308 genomics scRNA-Seq (**Fig. 6A**).

309 The integrated data identified 13 individual clusters, which we annotated according to
310 published marker gene expression (**Fig. 6B, S6A**)^{16,17}. We further sub-structured the HSPC
311 cluster and annotated 4 either immature (naïve) or differentiation-prone cell states (**Fig. 6C,**
312 **S6B**)^{16,17}. In line with the *Cdk6*^{KM/KM} HSC subcluster (**Fig. 1D**), the Palbociclib treated sample
313 showed a relative increase in cell number of the naïve subcluster compared to Ctrl (**Fig. 6D**).
314 To study the above defined HSC mediators regulated by CDK6 and MAZ (**Fig. 5G-H**), we
315 analysed the expression of these genes in the naïve subcluster (**Fig. 6E, S6C**). Top genes
316 identified in **Fig. 5H** including *Runx1*, *Cd53*, *Stat3*, *Mlec* and *Cdkn1b*, were found among the
317 top upregulated genes in the naïve Palbociclib treated subcluster compared to control.
318 To compare Palbociclib treated LSK cells with CDK6 kinase-inactive cells, we performed an
319 *in vivo* homing assay. CD45.2⁺ *Cdk6*^{+/+} LSK cells pre-treated with Palbociclib or control were
320 injected *i.v.* into CD45.1⁺ recipient mice (**Fig. S6D-E**). 18 hours upon injection, significantly
321 more HSC/MPP1 cells homed in the BM of the Palbociclib pre-treated setting, while LSK
322 cells remained unchanged. MPP2 cells were increased upon Palbociclib treatment, whereas
323 MPP3-4 were unaltered.
324 To validate the effects of CDK6 kinase inhibition on the colony-forming potential of HSPCs,
325 we performed serial plating assays with Palbociclib (**Fig. S6F**). Palbociclib treatment resulted
326 in increased colony and LSK cell numbers and decreased differentiated cells from the second
327 round of plating onwards.
328 *In vivo* treatment with Palbociclib every 24 hours over 10 days resulted in a higher percentage
329 of HSC/MPP1-MPP2 cells and reduced MPP3/4 cells in the BM (**Fig. 6F,G, S6G-H**).
330 Reduced myeloid cells in the BM confirmed the effectiveness of the treatment (**Fig. S6I**)²⁹.
331 HSC/MPP1 cells were embedded for a serial plating assay. Upon the second round of plating,
332 colony and LSK cell numbers of Palbociclib treated mice were enhanced (**Fig. 6H and S6J-**
333 **K**).

334 In combination with a MAZ knockdown, the colony numbers were reduced in the Palbociclib
335 and control condition whereas the LSK cells were reduced in the Palbociclib samples (**Fig.**
336 **S6L-M**).

337 Further, we treated freshly isolated LSK cells either with Palbociclib (CD45.2) or PBS
338 (CD45.1) and injected in a 1:1 ratio together with carrier bone marrow cells (GFP+) into
339 lethally irradiated recipient mice (**Fig. 6I**). After 16 weeks, Palbociclib treated HSC/MPP1
340 cells showed a competitive advantage (**Fig. 6J-K, S6N-O**).

341 To test the effect of Palbociclib in a human setting. CD34⁺ cord blood cells were plated with
342 either Palbociclib or control in methylcellulose for serial plating assays (**Fig. 6L**).
343 CD34⁺CD38⁻ cells were enriched with Palbociclib (**Fig. 6M-N**). Percentage of CD11b⁺ cells
344 was unaltered (**Fig. S6P**).

345 Taken together, we show that sustaining kinase-independent functions of CDK6 in HSCs
346 enables enhanced long-term capacity, which is reflected in a specific transcriptional pattern.
347 Kinase-inactivated CDK6 regulates quiescent and activated stem cell gene sets at least
348 partially with NFY-A and MAZ.

349

350 Discussion

351 The function of the hematopoietic system critically depends on the supply of new cells, which
352 are generated as needed by activation of the HSCs. Many patients suffer from hematopoietic
353 deficiencies, but we lack knowledge of when and how to intervene. HSCT is a potentially
354 curative therapy for various hematopoietic diseases. To enhance the success rate of HSCT, we
355 need to maintain stem cell potential and/or improve homing efficiency.

356 Homing is one of multiple processes involved in engraftment, which seems to be partially
357 influenced by CDK6³⁰. We propose that CDK4/6 kinase inhibitors could be used to maintain
358 cultured HSCs in their non-cycling and naïve state before they are transferred to the recipient.
359 While the canonical functions of both CDK4 and CDK6 are inhibited, the kinase-independent
360 functions of CDK6 are generally unaffected or even improved. CDK4/6 inhibitors cause a
361 transient arrest of the cell cycle in HSCs, thereby shield them from chemotherapy induced
362 damages³¹. We suggest that they could be used to treat donor-derived HSCs before HSCT to
363 inhibit their proliferation while improving their regeneration and homing potential.

364 Critical functions of CDK6 have been described in human cord blood cells. CDK6 enforced
365 expression in long-term (LT) HSCs leads to an increased cell division and those cells acquire
366 a competitive advantage which is suggested to be independent of cyclin expression³². Loss of
367 CDK6 in HSCs inhibits the cells' exit from dormancy upon activation¹³. We now demonstrate
368 that kinase-inactivated CDK6 influences the transcription of a set of genes to enhance HSC
369 functionality upon long-term activation. These kinase-independent functions of CDK6 might
370 partially explain the effects of LT-HSCs with enforced CDK6 expression, when cyclins are
371 not expressed yet^{32,33}. Loss of CDK6 in HSCs shows the opposite effect.

372 Hu et al. found 50% reduction in LSK cells of *Cdk6*^{-/-} and *Cdk6*^{KM/KM} mice compared to
373 *Cdk6*^{+/+} mice¹⁴, while our analysis failed to detect these differences. This could be caused by
374 Sca-1 expression changes. Sca-1 has previously been recognized to react to certain biological

375 stresses¹⁹, including mouse rearing facilities with different environmental background in a
376 similar way to the mouse genetic background.

377 CDK6 does not contain a DNA-binding domain but exerts its effects by interacting with
378 transcription factors. We have identified the transcription factors with which CDK6 interacts
379 to determine HSC self-renewal. In line with our data on leukemic cells,¹⁰ CDK6 interacts with
380 NFY-A in a kinase-dependent manner. The CDK6-NFY-A complex induces a gene set that
381 characterizes activated HSCs. CDK6 and CDK2 phosphorylate the DNA-binding domain of
382 NFY-A^{10,33,34}. We have shown that CDK6 interacts with NFY-A in *Cdk6*^{+/+} and *Cdk6*^{KM/KM}
383 HSPCs. We postulate that kinase-inactivated CDK6 inhibits NFY-A by interacting with it and
384 preventing its phosphorylation, thereby blocking the transcription of NFY-A-dependent genes
385 and suppressing the progression of HSCs to activated MPP1 cells. Knocking down NFY-A in
386 HSCs with kinase inactivated CDK6 leads to an increase in apoptosis, which was not seen in
387 HSCs with wildtype or lacking CDK6. This might be explained by the fact that both proteins
388 regulate p53-response^{10,24,25} and underline the importance of the delicate axis of CDK6 and
389 NFY-A in activated progenitor cells.

390 The transcription pattern of *Cdk6*^{KM/KM} HSCs upon transplantation directs the cells to a more
391 quiescent state. The HSC maintenance axis is characterized by a regulating complex including
392 CDK6 and MAZ. The critical role of kinase inactivated CDK6 and MAZ interaction is
393 supported by MAZ knockdown experiments in HSCs, as HSCs lose their self-renewal ability.

394 ChIP-Seq data of CDK6 and MAZ from leukemic B cells reveal a large set of common target
395 genes, showing that the role of CDK6 and MAZ is not restricted to healthy hematopoietic
396 cells. We speculate that the effect on MAZ might be due to a scaffolding function or to the
397 blockage of certain phosphorylation sites that are critical for transcriptional inactivation or
398 chromatin release. Similar to CTCF, MAZ interacts with a subset of cohesins to organize the
399 chromatin³⁵.

400 The transcription factor MAZ provides another possibility to balance differentiation. MAZ
401 binds the promoters of genes related to erythroid differentiation. It is highly expressed in
402 several cancers and regulates angiogenesis via VEGF, another known CDK6 target^{7,9,36-39}.
403 MAZ is also a cofactor of CTCF in embryonic stem cells, where it insulates active chromatin
404 at *Hox* clusters during differentiation³⁷. This function could explain the bias towards myeloid-
405 directed differentiation in *Cdk6*^{KM/KM} HSPCs, which suggests that CDK6 regulates *Hox* genes
406 and thereby differentiation together with MAZ and CTCF. We thus have evidence for a role
407 of CDK6 in regulation not only in the most naïve HSC compartment but also in early
408 hematopoietic progenitors.

409 Our data point at a regulation of NFY-A and MAZ by CDK6 which is important for the long-
410 term repopulation capability of HSCs. Our results present a strategy to enhance the success of
411 HSCTs by pre-treating HSCs with CDK4/6 kinase inhibitors. CDK4/6 kinase inhibitors are
412 used and tested for combinatorial cancer therapy^{7,40}. These treatments might bring an
413 advantage for healthy HSC fitness as a bystander of cancer therapy. We highlight CDK6 as a
414 major player in HSPCs and inactivation of the CDK6 kinase domain thus has dramatically
415 different consequences to loss of CDK6. In regards of the upcoming protein degrader
416 strategies, it is key to consider our data on HSCs lacking CDK6, showing a reduced HSC
417 potential for, any clinical trials.

418 **Acknowledgements:** The authors thank M. Ensfelder-Koperek, P. Kudweis, S. Fajmann, P.
419 Jodl, D. Werdenich and I. Dhrami for excellent technical support; G. Tebb for his excellent
420 knowledge and support in scientific writing; M. Milsom and F. Grebien for scientific
421 discussions; U. Ma for great technical support and the FACS facility MedUni Vienna for
422 experimental support; The Biomedical Sequencing Facility (BSF) at CeMM for NGS library
423 preparation, sequencing, and related bioinformatics analyses; This research was supported
424 using resources of the VetCore Facility (Mass Spectrometry) of the University of Veterinary
425 Medicine Vienna. Graphics were created with BioRender.com

426

427 **Authorship contributions:** Conceptualization, I.M.M., T.K., E.D., V.S., K.K.; formal
428 analysis, T.K., M.Z., R.G., G.H.; performing experiments I.M.M., E.D., S.K., L.G., M.P-M.,
429 A.S., M.F.; technical support U.M., L.E.S., N.K; resources: M.M.; A.F., E.Z-B.; writing,
430 I.M.M., E.D., T.K., K.K.; supervision, V.S., K.K.

431

432 **Disclosure of Conflicts of Interest:** The authors declare no competing interests.

433

434 **Funding:** This work was supported by the European Research Council (ERC) under the
435 European Union's Horizon 2020 research and innovation program grant agreement No
436 694354. This research was funded in whole or in part by the Austrian Science Fund (FWF)
437 [SFB-F6101, P 31773]. For open access purposes, the author has applied a CC BY public
438 copyright license to any author-accepted manuscript version arising from this submission.

439

- 441 1. Orkin SH, Zon LI. Hematopoiesis: An Evolving Paradigm for Stem Cell Biology. *Cell*.
442 2008;132(4):631–644.
- 443 2. Wilson A, Laurenti E, Oser G, et al. Hematopoietic Stem Cells Reversibly Switch from
444 Dormancy to Self-Renewal during Homeostasis and Repair. *Cell*. 2008;135(6):1118–
445 1129.
- 446 3. Mayer IM, Hoelbl-Kovacic A, Sexl V, Doma E. Isolation, Maintenance and Expansion of
447 Adult Hematopoietic Stem/Progenitor Cells and Leukemic Stem Cells. *Cancers*.
448 2022;14(7):1723.
- 449 4. Bazinet A, Popradi G. A General Practitioner’s Guide to Hematopoietic Stem-cell
450 Transplantation. *Current Oncology*. 2019;26(3):187–191.
- 451 5. Yanada M. The evolving concept of indications for allogeneic hematopoietic cell
452 transplantation during first complete remission of acute myeloid leukemia. *Bone Marrow*
453 *Transplant*. 2021;56(6):1257–1265.
- 454 6. Laurenti E, Göttgens B. From haematopoietic stem cells to complex differentiation
455 landscapes. *Nature*. 2018;553(7689):418–426.
- 456 7. Nebenfuehr S, Kollmann K, Sexl V. The role of CDK6 in cancer. *Int. J. Cancer*.
457 2020;147(11):2988–2995.
- 458 8. Handschick K, Beuerlein K, Jurida L, et al. Cyclin-Dependent Kinase 6 Is a Chromatin-
459 Bound Cofactor for NF-κB-Dependent Gene Expression. *Molecular Cell*. 2014;53(4):682.
- 460 9. Kollmann K, Heller G, Schneckenleithner C, et al. A Kinase-Independent Function of
461 CDK6 Links the Cell Cycle to Tumor Angiogenesis. *Cancer Cell*. 2013;24(2):167–181.
- 462 10. Bellutti F, Tigan A-S, Nebenfuehr S, et al. CDK6 Antagonizes p53-Induced Responses
463 during Tumorigenesis. *Cancer Discov*. 2018;8(7):884–897.
- 464 11. Uras IZ, Maurer B, Nivarthi H, et al. CDK6 coordinates JAK2V617F mutant MPN via
465 NF-κB and apoptotic networks. *Blood*. 2019; 11;133(15):1677–1690
- 466 12. Klein K, Witalisz-Siepracka A, Gotthardt D, et al. T Cell-Intrinsic CDK6 Is Dispensable
467 for Anti-Viral and Anti-Tumor Responses In Vivo. *Front. Immunol*. 2021;12:650977.
- 468 13. Scheicher R, Hoelbl-Kovacic A, Bellutti F, et al. CDK6 as a key regulator of
469 hematopoietic and leukemic stem cell activation. *Blood*. 2015;125(1):90–101.
- 470 14. Hu MG, Deshpande A, Schlichting N, et al. CDK6 kinase activity is required for
471 thymocyte development. *Blood*. 2011;117(23):6120–6131.
- 472 15. Malumbres M, Sotillo R, Santamaría D, et al. Mammalian Cells Cycle without the D-
473 Type Cyclin-Dependent Kinases Cdk4 and Cdk6. *Cell*. 2004;118(4):493–504.
- 474 16. Giladi A, Paul F, Herzog Y, et al. Single-cell characterization of haematopoietic
475 progenitors and their trajectories in homeostasis and perturbed haematopoiesis. *Nat Cell*
476 *Biol*. 2018;20(7):836–846.
- 477 17. Rodriguez-Fraticelli AE, Weinreb C, Wang S-W, et al. Single-cell lineage tracing unveils
478 a role for TCF15 in haematopoiesis. *Nature*. 2020;583(7817):585–589.
- 479 18. Venezia TA, Merchant AA, Ramos CA, et al. Molecular Signatures of Proliferation and
480 Quiescence in Hematopoietic Stem Cells. *PLoS Biol*. 2004;2(10):e301.
- 481 19. Kanayama M, Izumi Y, Yamauchi Y, et al. CD86-based analysis enables observation of
482 bona fide hematopoietic responses. *Blood*. 2020;136(10):1144–1154.
- 483 20. Ito K, Turcotte R, Cui J, et al. Self-renewal of a purified *Tie2*⁺ hematopoietic stem cell
484 population relies on mitochondrial clearance. *Science*. 2016;354(6316):1156–1160.
- 485 21. Arai F, Hirao A, Ohmura M, et al. *Tie2*/Angiopoietin-1 Signaling Regulates
486 Hematopoietic Stem Cell Quiescence in the Bone Marrow Niche. *Cell*. 2004;118(2):149–
487 161.

- 488 22. Cabezas-Wallscheid N, Klimmeck D, Hansson J, et al. Identification of Regulatory
489 Networks in HSCs and Their Immediate Progeny via Integrated Proteome, Transcriptome,
490 and DNA Methylome Analysis. *Cell Stem Cell*. 2014;15(4):507–522.
- 491 23. Doma E, Mayer IM, Brandstoeffer T, et al. A robust approach for the generation of
492 functional hematopoietic progenitor cell lines to model leukemic transformation. *Blood*
493 *Advances*. 2021;5(1):39–53.
- 494 24. Gatta R, Dolfini D, Mantovani R. NF-Y joins E2Fs, p53 and other stress transcription
495 factors at the apoptosis table. *Cell Death Dis*. 2011;2(5):e162–e162.
- 496 25. Bungartz G, Land H, Scadden DT, Emerson SG. NF-Y is necessary for hematopoietic
497 stem cell proliferation and survival. *Blood*. 2012;119(6):1380–1389.
- 498 26. Pinto do O P. Expression of the LIM-homeobox gene LH2 generates immortalized Steel
499 factor-dependent multipotent hematopoietic precursors. *The EMBO Journal*.
500 1998;17(19):5744–5756.
- 501 27. Yue F, Cheng Y, Breschi A, et al. A comparative encyclopedia of DNA elements in the
502 mouse genome. *Nature*. 2014;515(7527):355–364.
- 503 28. Busch K, Klapproth K, Barile M, et al. Fundamental properties of unperturbed
504 haematopoiesis from stem cells in vivo. *Nature*. 2015;518(7540):542–546.
- 505 29. Bisi JE, Sorrentino JA, Jordan JL, et al. Preclinical development of G1T38: A novel,
506 potent and selective inhibitor of cyclin dependent kinases 4/6 for use as an oral
507 antineoplastic in patients with CDK4/6 sensitive tumors. *Oncotarget*. 2017;8(26):42343–
508 42358.
- 509 30. Lapidot T, Dar A, Kollet O. How do stem cells find their way home? *Blood*.
510 2005;106(6):1901–1910.
- 511 31. He S, Roberts PJ, Sorrentino JA, et al. Transient CDK4/6 inhibition protects
512 hematopoietic stem cells from chemotherapy-induced exhaustion. *Sci. Transl. Med*.
513 2017;9(387):eaal3986.
- 514 32. Laurenti E, Frelin C, Xie S, et al. CDK6 Levels Regulate Quiescence Exit in Human
515 Hematopoietic Stem Cells. *Cell Stem Cell*. 2015;16(3):302–313.
- 516 33. Farina A, Manni I, Fontemaggi G, et al. Down-regulation of cyclin B1 gene transcription
517 in terminally differentiated skeletal muscle cells is associated with loss of functional
518 CCAAT-binding NF-Y complex. *Oncogene*. 1999 6;18(18):2818–27.
- 519 34. Yun J, Chae H-D, Choi T-S, et al. Cdk2-dependent Phosphorylation of the NF-Y
520 Transcription Factor and Its Involvement in the p53-p21 Signaling Pathway. *Journal of*
521 *Biological Chemistry*. 2003;278(38):36966–36972.
- 522 35. Xiao T, Li X, Felsenfeld G. The Myc-associated zinc finger protein (MAZ) works
523 together with CTCF to control cohesin positioning and genome organization. *Proc. Natl.*
524 *Acad. Sci. U.S.A.* 2021;118(7):e2023127118.
- 525 36. Deen D, Butter F, Daniels DE, et al. Identification of the transcription factor MAZ as a
526 regulator of erythropoiesis. *Blood Advances*. 2021;5(15):3002–3015.
- 527 37. Ortabozkoyun H, Huang P-Y, Cho H, et al. CRISPR and biochemical screens identify
528 MAZ as a cofactor in CTCF-mediated insulation at Hox clusters. *Nat Genet*.
529 2022;54(2):202–212.
- 530 38. Triner D, Castillo C, Hakim JB, et al. Myc-Associated Zinc Finger Protein Regulates the
531 Proinflammatory Response in Colitis and Colon Cancer via STAT3 Signaling. *Molecular*
532 *and Cellular Biology*. 2018;38(22):e00386–18.
- 533 39. Yu Z-H, Lun S-M, He R, et al. Dual function of MAZ mediated by FOXF2 in basal-like
534 breast cancer: Promotion of proliferation and suppression of progression. *Cancer Letters*.
535 2017;402:142–152.
- 536 40. Fassl A, Geng Y, Sicinski P. CDK4 and CDK6 kinases: From basic science to cancer
537 therapy. *Science*. 2022;375(6577):eabc1495.

538

539

540 **Figure legends**

541 **Figure 1: CDK6 shapes the HSC transcriptomic landscape in a kinase-inactivated,**
542 **kinase -dependent and -independent manner**

543 (A) Flow cytometry analysis of isolated BM from *Cdk6*^{+/+}, *Cdk6*^{-/-} and *Cdk6*^{KM/KM} mice. Cell
544 numbers of HSCs (LSK [Lin⁻Sca-1⁺c-kit⁺] CD34⁻CD48⁻CD150⁺CD135⁻), MPP1 (LSK
545 CD34⁺CD48⁻CD150⁺CD135⁻), MPP2 (LSK CD48⁺CD150⁺) and MPP3/4 (LSK
546 CD48⁺CD150⁻), (n = 10; mean ± standard error of the mean [SEM]). (B) (top) Experimental
547 scheme of 10X Genomics scRNA-seq including flow cytometry sorting of LSK cells of
548 *Cdk6*^{+/+}, *Cdk6*^{-/-} and *Cdk6*^{KM/KM} BM. (bottom) Uniform Manifold Approximation and
549 Projection (UMAP) visualization of 11 LSK cell clusters. Colours indicate different clusters.
550 HSPC: Hematopoietic stem and progenitor cell, Cycle: Cell cycle, Myel: Myeloid, Lym:
551 Lymphoid, Rep: Replication (C) UMAP of 9 HSPC subclusters with colour code. MPP:
552 Multipotent progenitor, IFN: Interferon, Ery: Erythroid. (D) Bar chart of HSPC subcluster
553 size differences of either *Cdk6*^{-/-} or *Cdk6*^{KM/KM} compared to *Cdk6*^{+/+} control (Log₂FC of %
554 cluster sizes relative to *Cdk6*^{+/+}). (E) UMAP of *Cdk6*^{+/+}, *Cdk6*^{-/-} and *Cdk6*^{KM/KM} HSPC cluster.
555 Arrow indicates HSC subcluster. (F) (top) Nomenclature of kinase-inactivated, kinase-
556 dependent and loss of CDK6. (bottom) Venn diagrams showing number of genes of the HSC
557 subcluster uniquely or commonly upregulated (left) / downregulated (right) in *Cdk6*^{KM/KM} and
558 *Cdk6*^{-/-} compared to *Cdk6*^{+/+} (|Log₂FC| ≥ 0.3). (G) UMAP showing *Cdk6*^{+/+}, *Cdk6*^{-/-} and
559 *Cdk6*^{KM/KM} HSPCs overlayed with the HSC associated proliferation gene signature (Psig)¹⁸.
560 The 15% of cells with the lowest Psig score (compare methods) are indicated in blue. Violin
561 plots depicting Psig and HSC associated quiescent signature (Qsig) of all three genotypes.

562

563 **Figure 2: Kinase-inactivated CDK6 maintains HSPC potential upon long-term challenge**

564 (A) Experimental workflow of repetitive *in vivo* pI:pC injections followed by an *in vitro* serial
 565 plating assay of $Cdk6^{+/+}$, $Cdk6^{-/-}$ and $Cdk6^{KM/KM}$ BM cells. (B) Flow cytometry analysis of L⁻
 566 K⁺CD86⁺ and HSC-MPP1 (from L⁻K⁺CD86⁺) cells upon serial pI:pC injection (n ≥ 3, mean ±
 567 SEM). (C) Cell cycle distribution of HSC/MPP1 cells upon serial pI:pC treatment (n=5, mean
 568 ± SEM). (D) Representative flow cytometry plots showing serially plated LSK cells upon
 569 repetitive pI:pC treatment. (SP: serial plating) (E) Relative quantification of LSK cells during
 570 serial plating after repetitive *in vivo* pI:pC treatment (n = 3-6, mean ± SEM).

571 **Figure 3: Kinase-inactivated CDK6 enhances HSC homing and self-renewal**

572 (A) Top upregulated genes in dormant $Cdk6^{KM/KM}$ HSCs compared to $Cdk6^{+/+}$ and $Cdk6^{-/-}$
 573 cells from scRNA-seq. (B) Schematic representation of BM homing assay *in vivo*. (C) Flow
 574 cytometry analysis of homed CD45.2⁺ $Cdk6^{+/+}$, $Cdk6^{-/-}$ and $Cdk6^{KM/KM}$ LSK and HSC/MPP1
 575 of LSK cells 18h post-injection into CD45.1⁺ recipients (n ≥ 11 recipients and donors, mean ±
 576 SEM). (D) Serial BM transplantation workflow of $Cdk6^{+/+}$, $Cdk6^{-/-}$ and $Cdk6^{KM/KM}$ BM cells.
 577 (E) Representative flow cytometry plots of gated LSK cells over four rounds of
 578 transplantation (TP). (F, G) % of engrafted CD45.2⁺ $Cdk6^{+/+}$, $Cdk6^{-/-}$ and $Cdk6^{KM/KM}$ LSK and
 579 HSC/MPP1 cells over four rounds of transplantation. (H) Lineage distribution of engrafted
 580 CD45.2⁺ $Cdk6^{+/+}$, $Cdk6^{-/-}$ and $Cdk6^{KM/KM}$ BM cells (n = 3-6/genotype, mean ± SEM). (I)
 581 Experimental design competitive BM transplantation assay, depicting 1:1 ratio
 582 transplantation of CD45.1⁺ $Cdk6^{+/+}$ together with either CD45.2⁺ $Cdk6^{+/+}$ or $Cdk6^{KM/KM}$ BM
 583 into lethally irradiated recipient mice. (J) Endpoint analysis of competitive transplantation
 584 showing CD45.2⁺ $Cdk6^{+/+}$ and $Cdk6^{KM/KM}$ HSC/MPP1 cells (n = 7/group, mean ± SEM).

585 **Figure 4: Kinase-inactivated CDK6 balances quiescent and activated transcriptional**
 586 **programs of long-term HSCs**

587 (A) Experimental workflow of low-input RNA-seq of engrafted CD45.2⁺ HSC/MPP1 cells
588 after two serial rounds of transplantation. (B) Venn diagrams showing genes uniquely or
589 commonly upregulated (left) / downregulated (right) in *Cdk6*^{-/-} and *Cdk6*^{KM/KM} compared to
590 *Cdk6*^{+/+} HSC/MPP1 cells after two serial rounds of transplantation (n=3, |Log₂FC| ≥ 0.3,
591 adjusted p-value < 0.2). (C, D) Gene set enrichment analysis (GSEA) to test for the
592 enrichment of quiescent or activated stem cell gene sets in differentially expressed genes
593 coming from three analyses: HSC/MPP1 cells of *Cdk6*^{KM/KM} in comparison to *Cdk6*^{+/+} cells,
594 *Cdk6*^{KM/KM} compared to *Cdk6*^{-/-} or *Cdk6*^{-/-} compared to *Cdk6*^{+/+} after two serial rounds of
595 transplantation. (E, F) Transcription factor motif enrichment analysis of genes within the
596 activated stem cell gene set that are either upregulated in (E) *Cdk6*^{KM/KM} compared to *Cdk6*^{+/+}
597 HSC/MPP1 cells or (F) *Cdk6*^{-/-} compared to *Cdk6*^{+/+} HSC/MPP1 cells upon two serial rounds
598 of transplantation. (G) Subcellular fractionation of *Cdk6*^{+/+}, *Cdk6*^{-/-} and *Cdk6*^{KM/KM} HPC^{LSK}
599 cells, followed by western blot analysis of CDK6. Lamin B1/RCC1 served as nuclear, while
600 HSP-90 as a cytoplasmic marker. (H) Anti-NFY-A co-immunoprecipitation (co-IP) from
601 HPC^{LSK} *Cdk6*^{+/+}, *Cdk6*^{-/-} and *Cdk6*^{KM/KM} cell extracts followed by NFY-A and CDK6
602 immunoblotting. IN indicates the input lysate and SN indicates the supernatant after IP.
603 GAPDH served as loading control.

604 **Figure 5: Kinase-inactivated CDK6 and MAZ influence HSC maintenance**

605 (A-B) Transcription factor motif enrichment analysis of genes within the quiescence stem cell
606 gene set that are either upregulated in (A) *Cdk6*^{KM/KM} compared to *Cdk6*^{+/+} cells or (B) *Cdk6*^{-/-}
607 compared to *Cdk6*^{+/+} cells after two serial rounds of transplantation. (C) CDK6 interactome
608 analysis generated by nuclear CDK6-IP mass spectrometry analysis of HPC-7 cell lines
609 expressing either wildtype CDK6 or CDK6^{KM}. Dot plot illustrating all protein interactions
610 with CDK6 or CDK6^{KM} vs. CDK6^{-/-} (Log₂FC). Established CDK6 interactors are highlighted
611 in blue. Transcription factors interacting with CDK6^{KM} and analyzed from the CDK6^{KM}

612 specific motif analysis from Fig. S5A are highlighted in red. **(D)** Flow cytometry proximity
613 ligation assay of CDK6 and MAZ antibodies showing endogenous protein interaction in *ex*
614 *vivo* *Cdk6*^{+/+}, *Cdk6*^{-/-} and *Cdk6*^{KM/KM} HSC/MPP1 cells. Representative flow cytometry
615 histograms are depicted on the right. *Cdk6*^{-/-} cells, MAZ and CDK6 antibody only samples
616 served as controls. **(E)** Overlap of CDK6 ChIP-seq data from BCR/ABL^{p185+} cells with
617 published MAZ ChIP-seq data from CH12.LX mouse lymphoma cell line. **(F)** Annotation of
618 the genomic regions identified in the CDK6/MAZ ChIP-seq overlap. **(G)** CDK6/MAZ ChIP-
619 seq overlay (+2kb- -500b to TSS) with upregulated genes of *Cdk6*^{KM/KM} compared to *Cdk6*^{+/+}
620 dormant HSC subcluster genes (scRNA-seq FC ≥ 0.3). **(H)** Stem cell genes of *Cdk6*^{KM/KM} or
621 *Cdk6*^{-/-} cells compared to *Cdk6*^{+/+} cells with a CDK6-MAZ ChIP peak. **(I)** Experimental
622 design of siRNA MAZ knockdown assay +/- Palbociclib treatment in sorted LSK cells of
623 *Cdk6*^{+/+} and *Cdk6*^{KM/KM} mice. **(J, K)** Flow cytometry analysis of **(J)** HSC/MPP1 scramble
624 cells and **(K)** HSC/MPP1 cells of LSK cells upon MAZ knockdown +/- Palbociclib treatment
625 depicted as Log₂FC relative to corresponding scramble controls (n = 4 per genotype, mean ±
626 SEM).

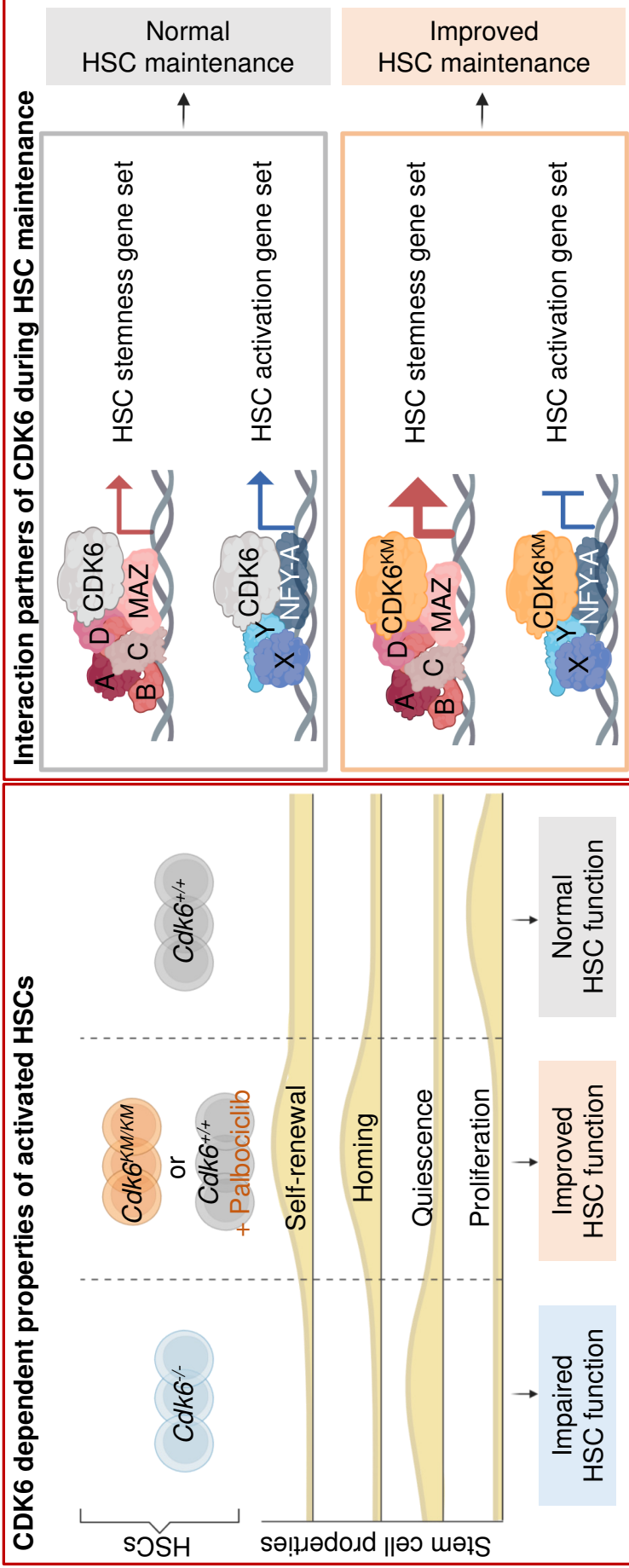
627 **Figure 6: CDK4/6 kinase inhibition protects HSC fitness**

628 **(A)** Experimental scheme of 10X Genomics scRNA-seq including flow cytometry sorting of
629 LSK cells followed by 24h cultivation with either PBS or Palbociclib. **(B)** UMAP
630 visualization of 13 LSK cell clusters. Colours indicate different clusters. Neutro: Neutrophil,
631 Dendr: Dendritic, Cycle: Cell cycle, M/L Cycle: Myeloid/Lymphoid cell cycle, Innate: Innate
632 lymphocyte, MK: Megakaryocyte, Ribos: Ribosomes, HSPC: Hematopoietic stem and
633 progenitor cell, Ery: Erythroid, Granu: Granulocyte, D/M: Dendritic/Macrophage. **(C)** UMAP
634 of 4 HSPC subclusters. Myel 1: Myeloid (Granulocyte), Myel 2: Dendritic, Myel 3:
635 Neutrophil, Naïve: Immature cells. **(D)** Bar chart of relative HSPC subcluster sizes of the PBS
636 or Palbociclib treated samples. **(E)** Heatmap of top 50 upregulated genes upon Palbociclib

637 treatment compared to control out of the 282 genes found in Fig. 5G. Errors indicate top
638 genes of Fig. 5H, also found in the Palbociclib comparison. **(F)** Experimental design to assess
639 *in vivo* Palbociclib treatment followed by an *in vitro* serial plating assay of sorted HSC/MPP1
640 cells. **(G)** Flow cytometry analysis of HSC/MPP1 cells and **(H)** serially plated LSK cell
641 numbers upon *in vivo* Palbociclib treatment ($n \geq 4$, mean \pm SEM). **(I)** Experimental design for
642 competitive BM transplantation assay. CD45.1⁺ control and Palbociclib treated (200nM)
643 CD45.2⁺ BM cells were transplanted in a 1:1 ratio into lethally irradiated recipient mice upon
644 72h of cultivation. **(J, K)** Endpoint analysis of engrafted BM LSK and HSC/MPP1 cells upon
645 Palbociclib treatment ($n = 7$ /group, mean \pm SEM). **(L)** Experimental overview of PBS or
646 Palbociclib treated human CD34⁺ cells followed by a serial plating assay. **(M, N)** Percentage
647 of CD34⁺CD38⁻ cells and mean fluorescence intensity [MFI] of CD34⁺ cells in 2 serial plating
648 rounds ($n = 3-4$ /treatment, mean \pm SEM).

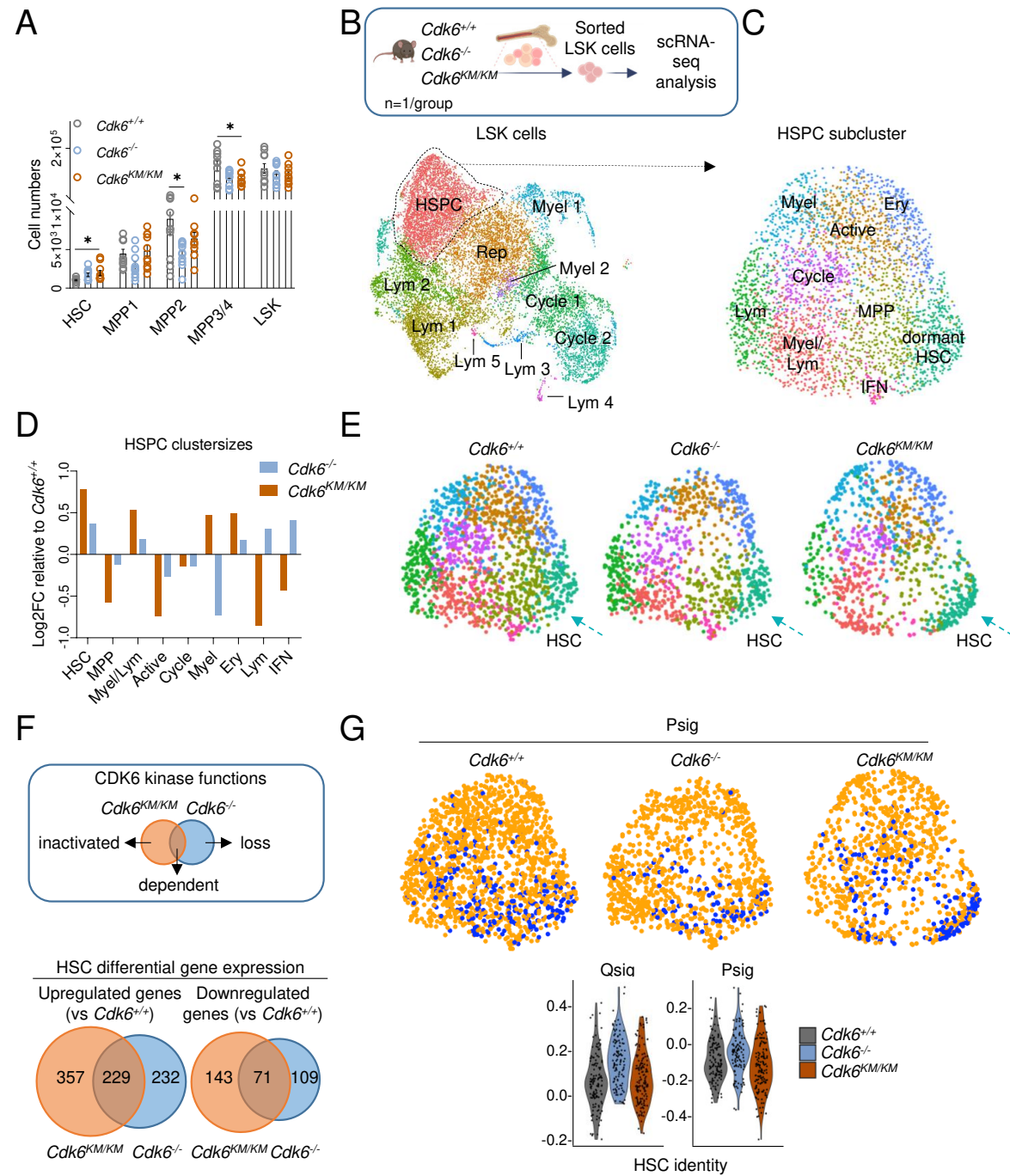
649

Kinase inactivated CDK6 in long-term HSC functionality



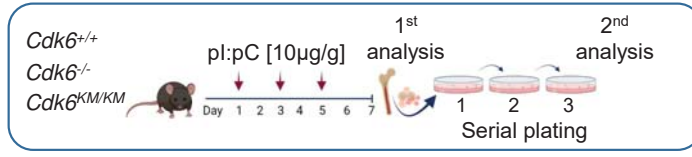
Conclusion: CDK6 balances self-renewal, homing, quiescence and proliferation in activated HSCs. Inhibiting CDK6 kinase function enhances long-term HSC functionality by a complex including CDK6 and MAZ, which activates an HSC maintenance specific transcriptional pattern.

Mayer et al. DOI

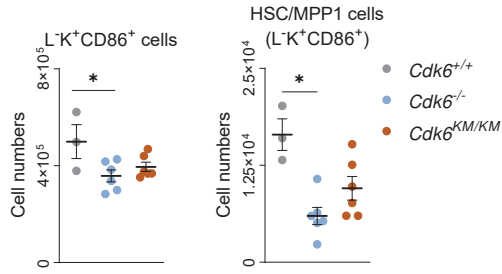


Revised Fig 2 Main Figure 2

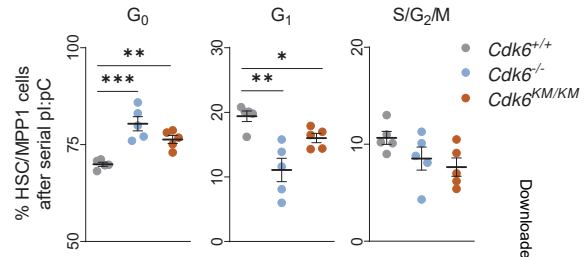
A



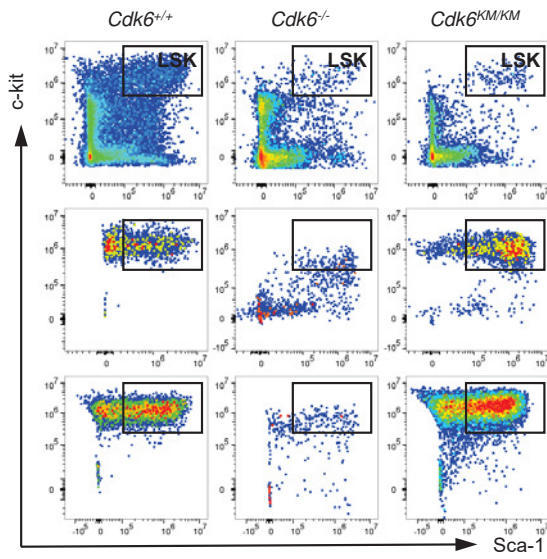
B 1st analysis:



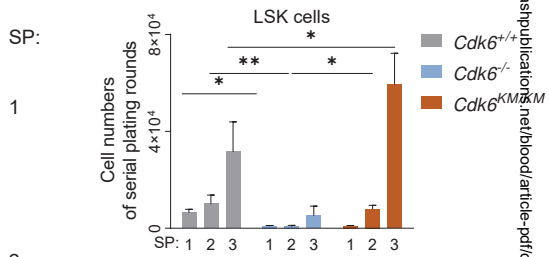
C



D 2nd analysis:

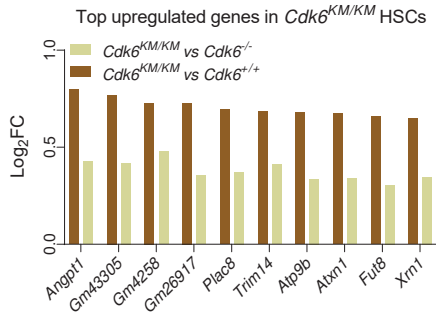


E



Revised Figure 3

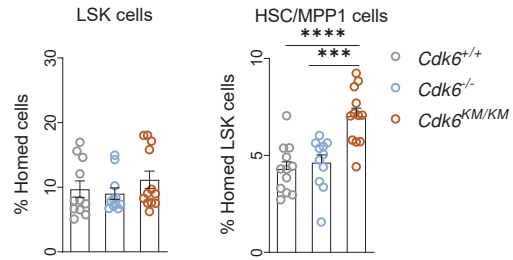
A



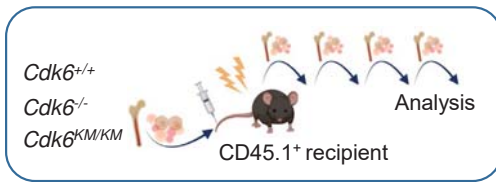
B



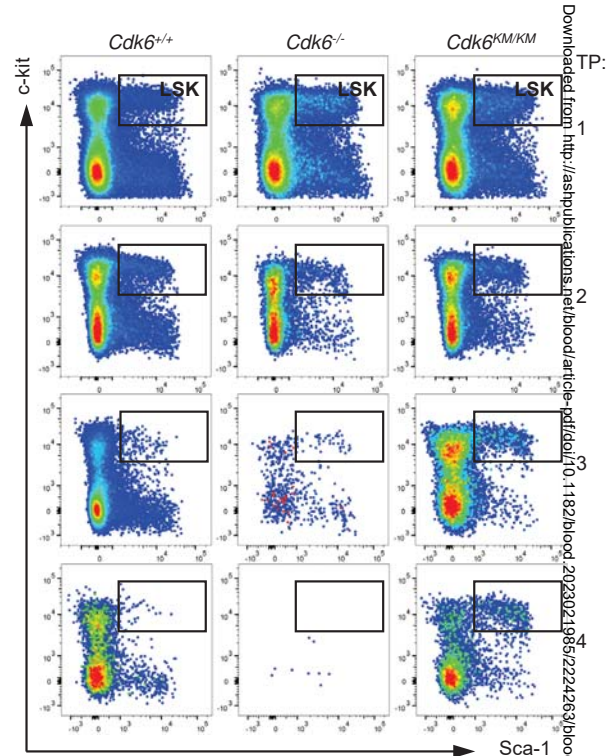
C



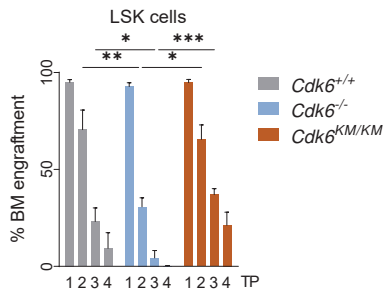
D



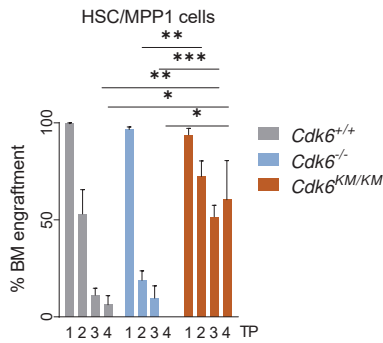
E



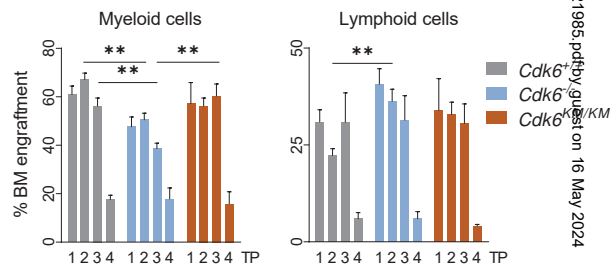
F



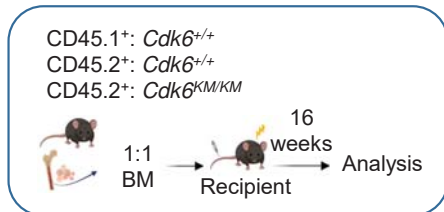
G



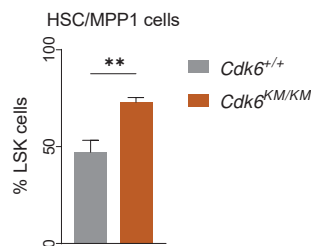
H



I



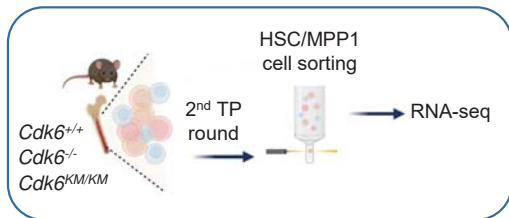
J



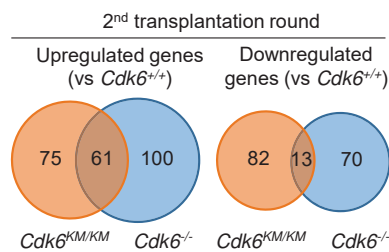
Downloaded from <http://ashpublications.org/blood/article-pdf/doi/10.1182/blood.2023021985/2224263/blood.2023021985.pdf> guest on 16 May 2024

Revised Figure 4

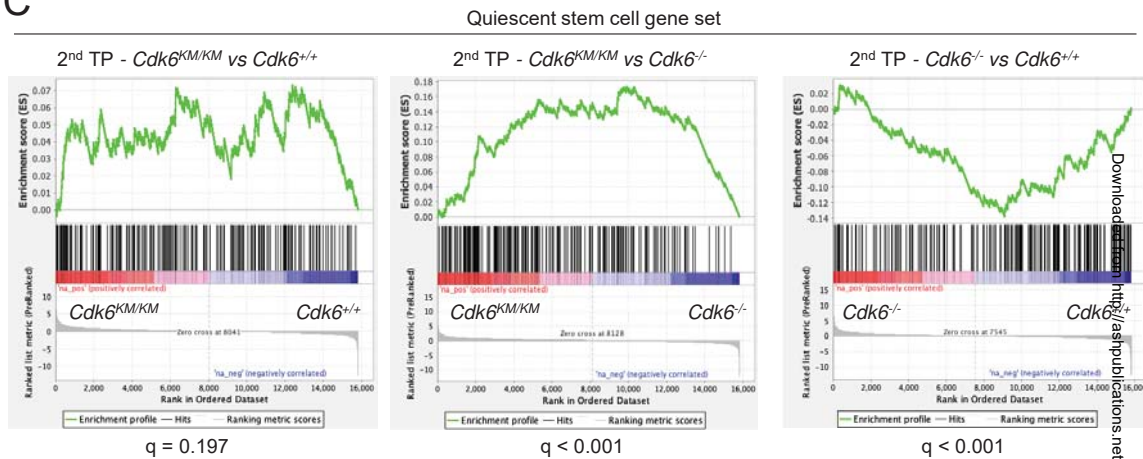
A



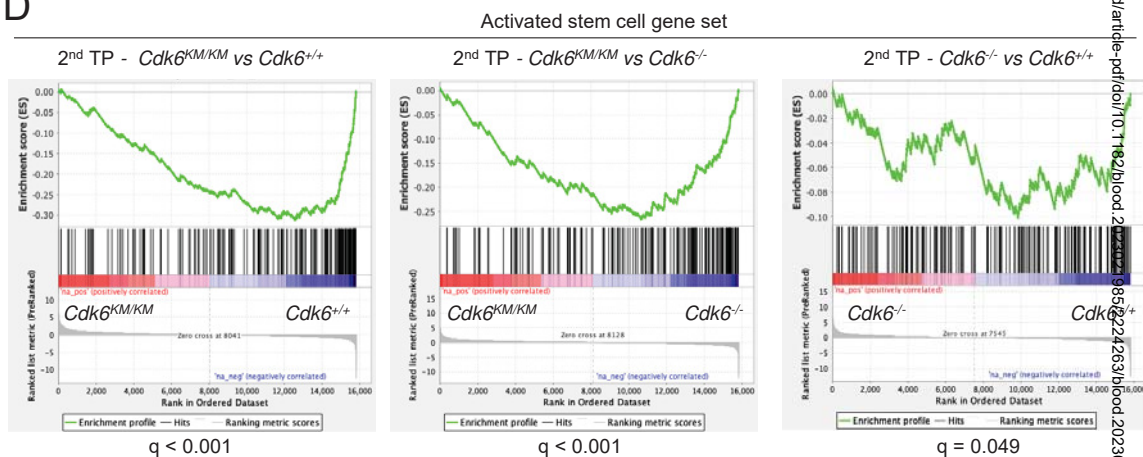
B



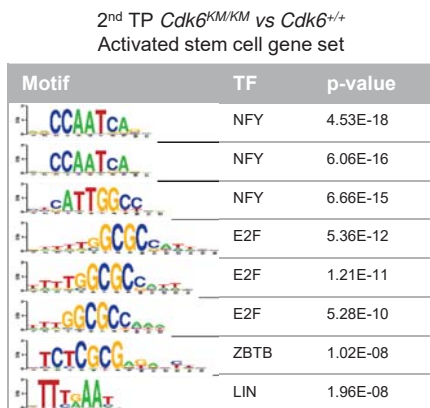
C



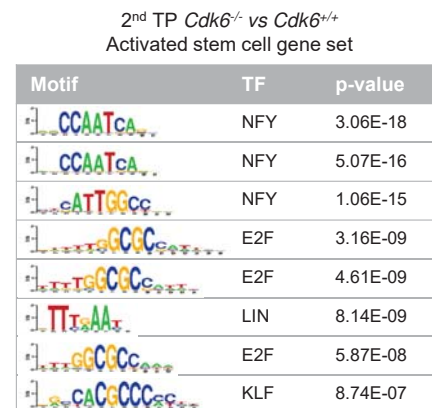
D



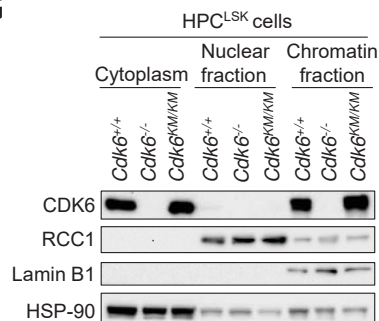
E



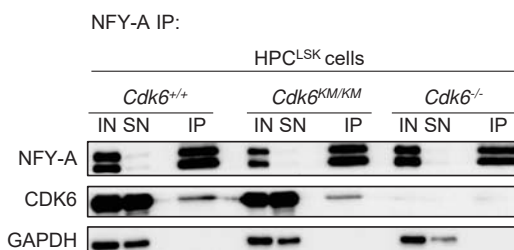
F



G

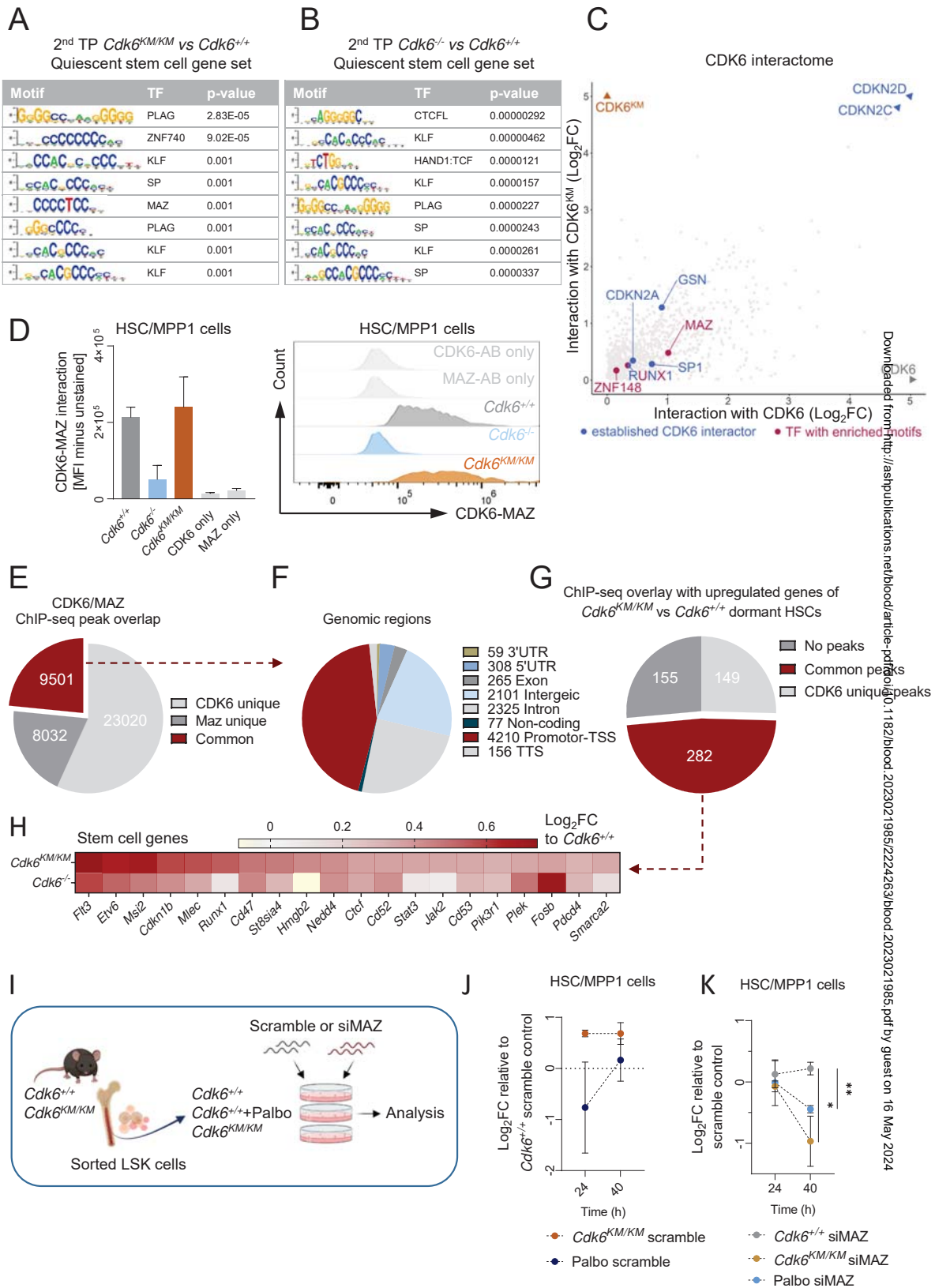


H

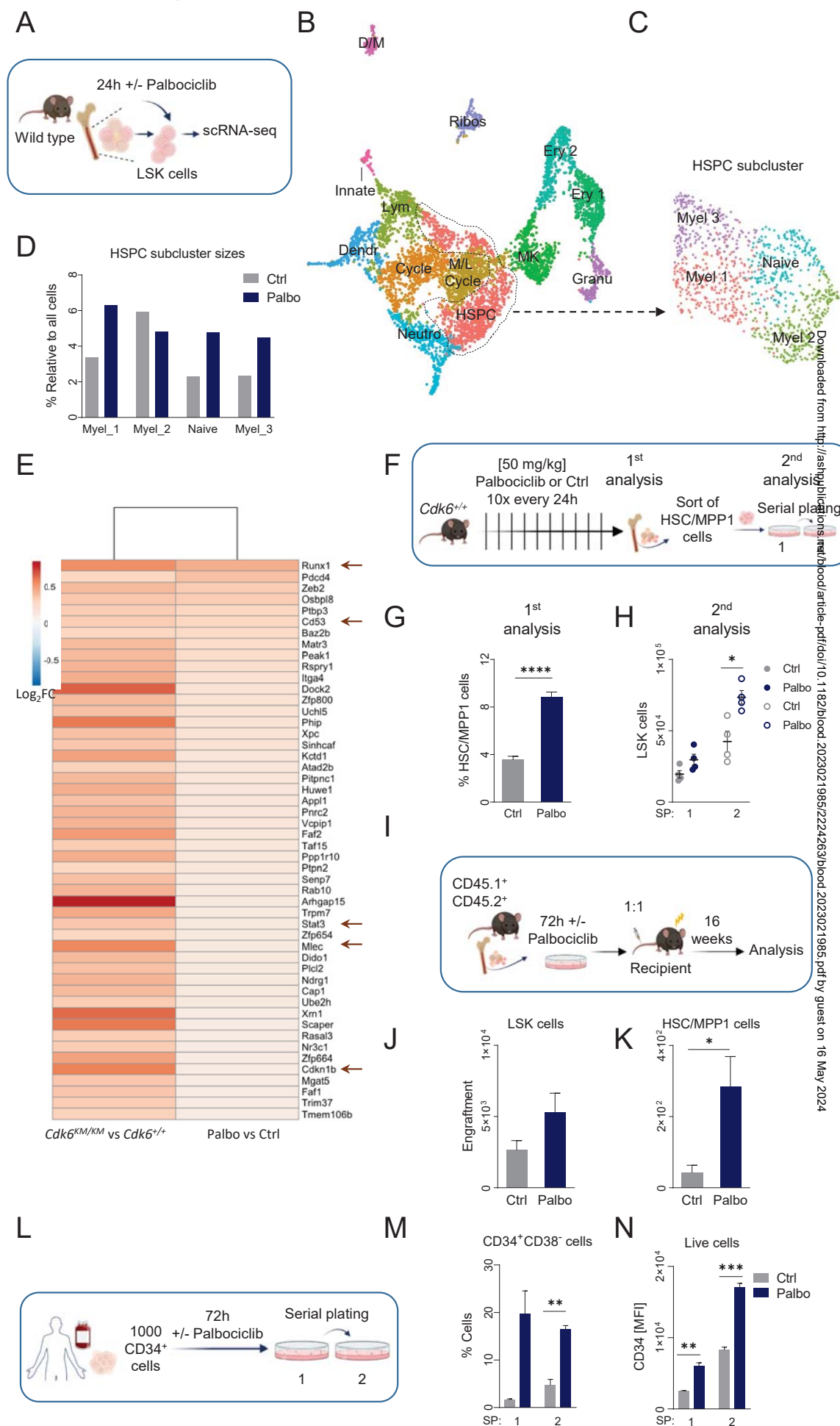


Downloaded from https://academic.oup.com/nb/article-pdf/doi/10.1093/nb/2023021985/pdf/doi/10.1093/nb/2023021985 by guest on 16 May 2024

Revised Figure 5



Revised Figure 3



Downloaded from <http://ashpublications.org/blood/article-pdf/doi/10.1182/blood.2023.02.1985/2224263/blood.2023.02.1985.pdf> by guest on 16 May 2024